Journal of Solid State Chemistry 231 (2015) 248–255

Contents lists available at ScienceDirect

Journal of Solid State Chemistry

journal homepage: www.elsevier.com/locate/jssc

The coexistence of cluster glass behavior and long-range ferromagnetic ordering in $La_{0.7}Sr_{0.25}Na_{0.05}Mn_{0.7}Ti_{0.3}O_3$ manganite

S.El. Kossi [a,*], S. Mnefgui [a], J. Dhahri [a], E.K. Hlil [b]

[a] Laboratoire de la matière condensée et des nanosciences, département de physique, faculté des sciences university de Monastir, 5019, Tunisia
[b] Institut Néel, CNRS et Université Joseph Fourier, BP 166,38042 Grenoble, France

ARTICLE INFO

Article history:
Received 31 May 2015
Received in revised form
22 July 2015
Accepted 20 August 2015
Available online 21 August 2015

Keywords:
Manganite
Magnetic
Critical phenomena
Magnetocaloric properties

ABSTRACT

The electron-doped $La_{0.7}Sr_{0.25}Na_{0.05}Mn_{0.7}Ti_{0.3}O_3$ ($LSNMTi_{0.3}$) sample was synthesized by a conventional solid-state reaction. Rietveld analysis of the X-ray diffraction (XRD) data showed that the compound crystallized in the space group $R\bar{3}c$. Magnetic characterization present a signature of a coexisting AFM–FM ordering and a cluster-glass phase. The M^2 vs. H/M curves prove that the samples exhibit a second-order magnetic phase transition and the critical properties near the ferromagnetic–paramagnetic phase transition temperature have been analyzed from data of the static magnetization measurements for the sample, through various techniques such as the modified Arrott plot and the critical isotherm analysis. The critical exponent values estimated from the isothermal magnetization measurements are found to be consistent and comparable to those predicted by the long-range mean-field theory.

1. Introduction

In recent years, magnetic materials as perovskite manganites ($RE^{3+}_{1-x}M^{2+}_{x}$)MnO_3 (RE=trivalent rare earth, M=divalent alkaline earth) with large magnetocaloric effect (MCE) and colossal magnetoresistance (CMR), have been extensively studied both experimentally and theoretically due to their great potential applications [1–6]. The close relation between transport and magnetism in these materials has been explained by many theories, such as doubles exchange (DE) interaction [7], Polaronic effects [8] and phase separation [9]. Among the fundamental questions which remain controversial is the universality class related to the ferromagnetic (FM) to paramagnetic (PM) in manganites [10,11]. The universality class does not depend on microscopic details of the system, but only on global information such as the dimension of order parameter and space. This practice has been extremely helpful in trying to discern the complexities of magnetic transitions in real systems [12]. Historically, the essential validity of the DE model Motome and Furukawa [13] argue, based on computational studies for DE models, that the FM–PM transition in these doped ferromagnetic manganites should belongs to the short-range Heisenberg universality class. Further computational studies on DE systems show that the transition may become discontinuous depending on doping level and competition with antiferromagnetic superexchange [14] similar to the Polaron model mentioned above. However, the relevance of these models for CMR manganites is an open problem. As pointed out above, it is possible that coupling of the magnetic subsystem to other modes may lead to a composite order parameter and different critical properties of the PM–FM transition. Experimental evidence for ferromagnetic clusters above the Curie temperature T_C [15], and the observations of inhomogeneity and phase separation [16] suggest the ferromagnetic long-range order may be established by percolation of magnetic regions when lowering temperature [17].

However, the experimental works on critical exponents are still controversial including the short-range Heisenberg interaction [18], the mean-fields values [19], the 3-D Ising values [20] and those which cannot be classified into any universality class ever known [21]. It is known, in perovskite manganite the critical exponent β varies in the 0.3–0.5 range. In addition, the reported values of γ vary between 1 and 1.4.

The doping of Ti at Mn site in $La_{0.7}Sr_{0.25}Na_{0.05}Mn_{1-x}Ti_xO_3$ compounds was systematically studied in our previous paper [22]. To summarize, the Ti^{4+} ions diluted the FM behavior of the system which is believed to be generated from the double-exchange (DE) interaction between electron spins of Mn^{3+} and Mn^{4+} ions. However, The Ti substitution creates some short-range ordered ferromagnetic clusters. By increasing the doping level of Ti^{4+} into the B site (Mn), we discovered the so-called magnetic frustration phenomenon in $La_{0.7}Sr_{0.25}Na_{0.05}Mn_{0.7}Ti_{0.3}O_3$, revealing a superposition of both FM and antiferromagnetic (AFM) interaction. To further investigate this phenomenon, this work studies the magnetic inhomogeneity and its impact on the critical behavior of $La_{0.7}Sr_{0.25}Na_{0.05}Mn_{0.7}Ti_{0.3}O_3$ sample near the ferromagnetic–

* Corresponding author. Fax: +216 73500278.
E-mail address: safwene666@hotmail.com (S.El. Kossi).

http://dx.doi.org/10.1016/j.jssc.2015.08.027
0022-4596/

paramagnetic phase transition temperature by the analyzing isothermal magnetization data. Using the Modified Arrott plots (MAPs), we point out that the critical phenomena near the PM–FM transition in this perovskite is described better by the long-range mean-field model.

2. Materials and methods

In this study, the $LSNMTi_{0.3}$ compound was prepared by the conventional solid state reaction described in our previous work [23]. Phase purity, homogeneity and cell dimensions were determined by powder X-ray diffraction (XRD) at room temperature. Structural analysis was carried out using the standard Rietveld method. The amount of Mn^{4+} ions has been quantitatively checked by iodometric titration. Magnetizations (M) vs. temperature (T) were measured using BS1 and BS2 magnetometer and the isotherm magnetization vs. magnetic field ($\mu_0 H$) was recorded by the SQUID-VSM system. The latter were measured in the range of 0–5 T and with a temperature interval of 3 K in the vicinity of the Curie temperature (T_C). Moreover, the magnetic entropy changes based on Maxwell relation were calculated from the magnetization data.

3. Scaling analysis

According to the scaling hypothesis, the critical behavior of a magnetic system showing a second-order magnetic phase transition near the Curie point is characterized by a set of critical exponents, β (the spontaneous magnetization exponent), γ (the isothermal magnetic susceptibility exponent) and δ (the critical isotherm exponent). Mathematically, the scaling hypothesis suggests the following powder-law relation near the critical region defined by [24, 25]:

$$M_S = \lim_{H\to 0}(M) = M_0(-\varepsilon)^{\beta},\ \varepsilon < 0\ T < T_C \tag{1}$$

$$\chi^{-1} = \lim_{H\to 0}(H/M) = (h_0/m_0)\varepsilon^{\gamma},\ \varepsilon > 0\ \ T > T_C \tag{2}$$

$$M = DH^{1/\delta},\ \varepsilon = 0\ \ T = T_C \tag{3}$$

Where M_0, h_0 and D are the critical amplitudes, and $\varepsilon = (T - T_C)/T_C$ is the reduced temperature. $M_s(T)$, χ_0^{-1} (T) and H are the spontaneous magnetization, the inverse initial susceptibility and the demagnetization adjusted applied magnetic field, respectively.

Another independent way to determine the exponent β and γ is available as well. It uses the scaling theory, which predicts the existence of a reduced equation of state given by:

$$M(H, \varepsilon) = |\varepsilon|^{\beta} f \pm\ (H/\ |\varepsilon|^{\beta+\gamma}) \tag{4}$$

Where f_+ for $T > T_C$ and f_- for $T < T_C$ are regular analytical functions. This equation implies that for the scaling relations and right choice of β, γ and δ values, the scaled $M/\ |\varepsilon|^{\beta}$ plotted as a function of the scaled $H/\ |\varepsilon|^{\beta+\gamma}$ will fall in tow universal curve, one above T_C and the other below T_C.

4. Results and discussion

4.1. Structural properties

The crystallographic structure and lattice parameters of $LSNMTi_{0.3}$ were determined using X-ray powder diffraction (XRD).

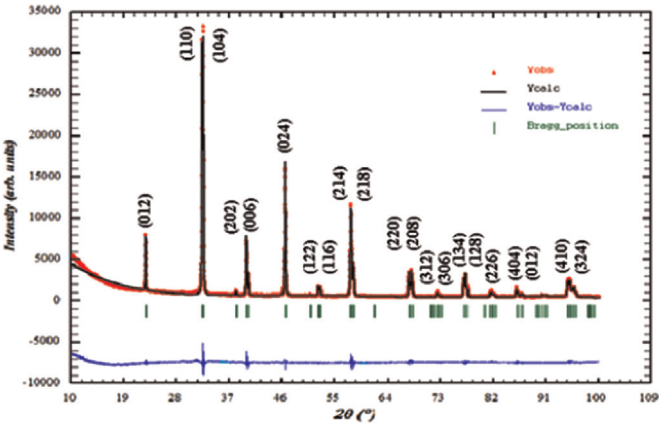

Fig. 1. observed (open symbols) and calculated (solid lines) X-ray diffraction pattern for $LSNMTi_{0.3}$. Position for the Bragg reflections is marked by vertical bars. Differences between the observed and the calculated intensities are shown at the bottom of the figure.

XRD patterns were recorded on an XPERT-PRO diffractometer equipped with PIXcel detector, using a graphite monochromatized Cuk_{α} radiation ($\lambda_{Cuk\alpha} = 1.54$ Å). in the angular range of 10–100° with a step size of 0.017° and a counting time of 18 s per step. The data were analyzed with the Rietveld refinement technique [26] using FullProf code [27]. The process of refinement was started with scale and background parameters followed by the unit cell parameters. Then, the peak asymmetry and preferred orientation corrections were applied. Finally, positional parameters and individual isotropic parameters were refined. The atomic occupations were set in term of formula and not refined in this work. Fig. 1 shows the room temperature X-ray diffraction (XRD) pattern of the synthesized $LSNMTi_{0.3}$ sample including the observed and calculated profile as well as the difference profile. As can be seen from this figure, the sample is in a single phase without any detectable secondary phase and can be indexed according to the rhombohedral perovskite structure with space group R-3c (No. 167), in which the (La,Sr,Na) atoms are at 6a (0,0,1/4) positions, Mn at 6b (0,0,0) and O at 18e (x,0,1/4). The difference observed between the intensities of the measured and calculated diffraction pattern can be attributed to the existence of a preferential orientation of the crystallites in the sample. Detailed results of the structural parameters deduced from the refinement are summarized in the Table. 1. One can see in this table and in our previous paper [22] that all the structural parameters including cell parameters, and the unit cell volume V of the Ti-doped samples increase with increasing of the Ti doping level. It is worth noticing that the substitution of Titanium at B-site, causes a distortion of the hexagonal structure by an elongation along both the a and c axes and therefore an increase of the cell volume. This is reliable with the fact that ionic radii of Ti^{4+} ($r_{Ti}{}^{4+} = 0.605$ Å) is higher than the manganese Mn^{4+} ($r_{Mn}{}^{4+} = 0.53$ Å). The changes in the lattice parameters are insignificant indicating that increase in Ti substitution did not produce any significant distortion in the crystal structure.

The evolution of hexagonal setting of the R-3c space group as a function of the Titanium content x can be fitted by a linear law. It was found that the slope of the straight line $a(x)$ parameter ($\Delta a/\Delta x = 0.094 \pm 0.001$ Å) and $c(x)$ ($\Delta c/\Delta x = 0.25 \pm 0.001$ Å), as it has been observed in other rare-earth manganites. This kind of behavior has been attributed to the tilting of MnO_6 octahedra in R-3c perovskite structure. In order to investigate the sample homogeneity in more detail, we have used the lattice parameter c to estimate the average value of x with its standard deviation and we find $\Delta x = 0.31 \pm 0.002$ Å. Note that this value confirms the cationic compositions of the samples.